CHARACTERIZATION OF THE SIZE AND SPATIAL PARTICLE DISTRIBUTIONS IN ALUMINIUM ALLOYS

O. Daaland[1] and E. Nes[2]
1. Hydro Aluminium a.s, R & D Centre, Karmøy, N-4265 Håvik, Norway
2. Norwegian Institute of Technology, Department of Metallurgy, 7034 Trondheim, Norway

Abstract

In the present investigation a two-dimensional tesselation procedure has been used in order to characterize the particle distribution in a commercial aluminium alloy. By applying this procedure it was possible to quantify the degree of particle clustering in samples rolled to different strain levels. A characteristic aspect seems to be a transition from a rather non-uniform spatial distribution at low rolling strains, towards a more or less random distribution at high strains. A simple model is proposed which explains the development of the spatial particle distribution as a function of rolling strain.

Introduction

Particle stimulated nucleation (PSN) of recrystallization is regarded as an important softening mechanism during annealing of commercial aluminium alloys. Modelling recrystallization in a situation where PSN is a dominating mechanism requires knowledge of the size distribution of particles. For successful prediction it is in addition necessary to know how the paticles are spatial organised in the structure. A description of the spatial distribution of particles in a structure may be obtained by the construction of so-called "Voronoi patterns", a problem studied initially by Dirichlet [1] and Voronoi [2]. By this approach the material is subdivided into cells constructed around each particle, and the geometry of the cells is subsequently analysed. The Voronoi polygons produced from a two dimensional particle pattern will be enclosed by the halfway lines between the particle and its neighbours. In the present investigation a procedure based on the same principles as the Dirichlet or Voronoi routines has been utilised to characterise the spatial, two dimensional particle distribution.

Material

The material analysed in this study was a commercial Al-Mn-Mg alloy, which was hot and/or cold rolled to different levels of strain. For each strain condition samples were cut in the longitudinal transverse section of the sheet, and the particles were analysed with respect to size and spatial distribution both in the surface and centre section of the sheet.

Experimental

Commercial aluminium alloys contain particles with a very wide size distribution. The particle sizes of interest in this investigation range from 1 μm to about 10 μm in diameter. This size range can be characterised adequately in a scanning electron microscope by a FDC-analysis (Feature, Detection and Classification).

Tessellation procedure The procedure applied for spatial particle characterisation uses the FDC-analysis described above, provided by the LINK eXL EDS image analyser. The principle of the procedure is shown in Fig. 1. Using the same metallographic samples as in the particle size characterisation, the FDC-analysis is performed in such a way that only particles larger than 1 μm are detected. Figure 1a shows the particle structure of large particles obtained from a randomly selected location (longitudinal transverse mid-section) of the sheet. The particle structure has been transmitted from the SEM-unit to the image analyser. Each particle is then shrunk to its centre of gravity (Fig. 1b) before the particles are allowed to "swell" at an isotropic and constant growth rate, until impingement (Fig. 1c). In order to avoid edge effects, all "grains" which touch the edge of the measurement frame are removed from the selection, as shown in Fig. 1d. It is emphasised that all particles (or points) start to grow at the same instant (t=0), i.e. a 2-dimensional site saturation kinetic situation, and grow with an isotropic and constant growth rate until impingement.
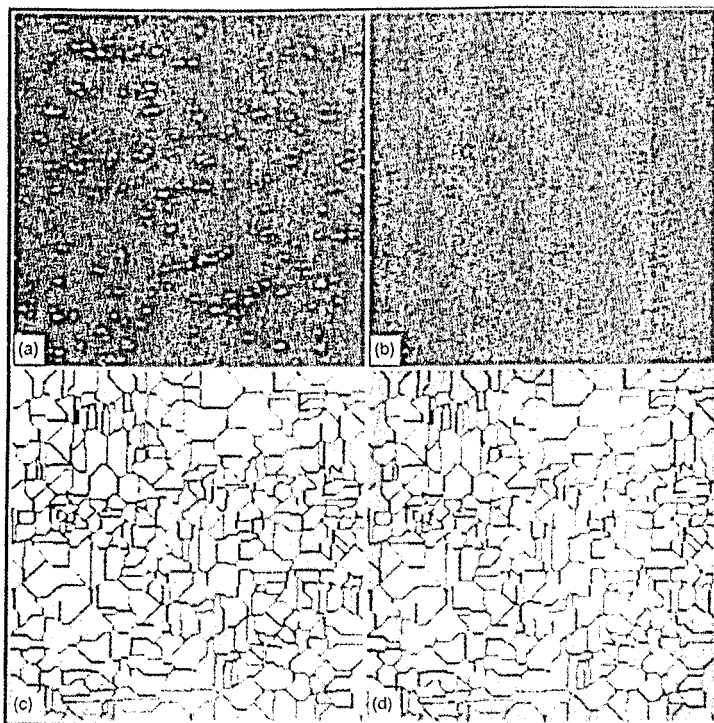

Figure 1. The principles of the tessellation procedure applied (for details see the text).

The kinetics as well as the "grain structure" evolution can be followed during the transformation. The tessellation procedure can be stopped at any arbitrarily selected time and the fraction "transformed" measured using the LINK-software. In such a way transformation curves can be obtained and the kinetics described in terms of the general transformation equation given below :

$$X_v = 1 - \exp(-kt^n) \qquad (1)$$

where k is a constant and the exponent n is referred to as the JMAK-exponent.

It should be noted that with a random distribution of "nucleation"-sites in 2 dimensions, site saturation nucleation kinetics, and an isotropic and constant growth rate, classical JMAK-theory predicts the JMAK-exponent to equal 2. However, if the sites are non-random distributed the JMAK-exponent remains constant, but with a value less than 2 [3]. Accordingly, determination of the JMAK-exponent (or n-value) using this procedure therefore provides a quantitative measure that enables us to estimate how far away the particles are from being randomly distributed in space. Another measure of the deviation from randomness is obtained by comparing the Voronoi-cell size distribution to that obtained from Voronoi-cells generated from a random distribution of sites.

Results and discussion

Size distribution of particles Figure 2 shows the cumulative size distributions of particles at different strain levels. In the as-cast and homogenised material a rather broad size distribution is found with an average particle diameter of 4.7 μm. During hot rolling the eutectic network of particles formed during solidification is fragmented and broken up, leading to a much more
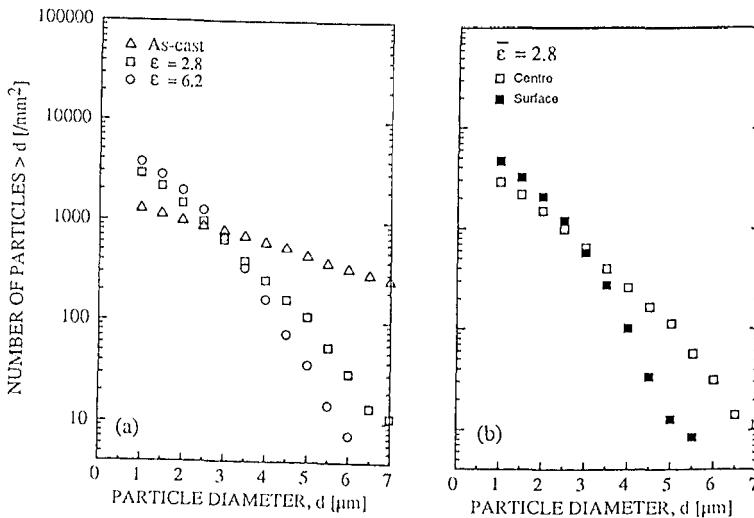

Figure 2. Cumulative size distribution of particles.

narrow size distribution (steeper cumulative size distribution). At a strain of $\bar{\varepsilon}$ = 2.8 the amount of particles larger than 3 μm are seen to be drastically reduced with a corresponding increase in the number of particles being less than 3 μm. As can be seen in Fig. 2b, there is a significant variation

in the size distribution of the intermetallics from the surface to the centre of the slab at this strain. Heavier rolling reductions ($\bar{\varepsilon}$ = 6.2) shift the distribution towards smaller sizes, resulting in an average particle diameter of 1.9 µm at the exit hot rolling gauge. However, no significant difference in the size distribution is observed when comparing the surface and centre region at this strain level.

Spatial distribution of particles (in 2D) Back scattered electron images of the particle structure in the Al1Mn1Mg slab/sheet mid-section after various stages of processing are shown in Fig. 3. The spatial distribution of the particles are seen to vary considerably at the different processing steps. In the as-cast and homogenised condition (Fig. 3a) a characteristic aspect is the network of intermetallics $Al_6(Mn,Fe)$ and $Al_{12}(Mn,Fe)_3Si_2$ describing the cell boundaries formed during solidification. At early stages of hot rolling (Fig. 3b) the particles build up in distinct layers giving a rather non-uniform distribution. However, at higher strain levels (Fig. 3c) a more uniform spatial distribution of the particles seems to be the case.

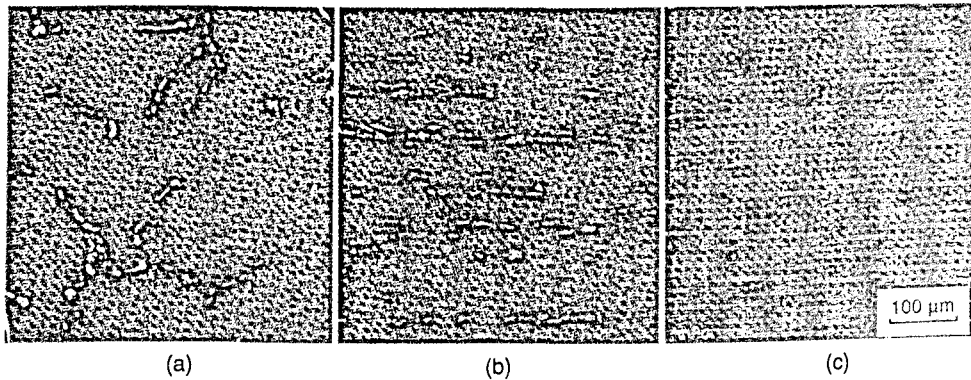(a)   (b)   (c)

Figure 3. SEM-micrographs showing the particle structure at different levels of processing. (a) As-cast and homogenised condition, (b) hot rolled to $\bar{\varepsilon}$ = 2.8, (c) hot rolled to $\bar{\varepsilon}$ = 6.2.

An example of a tessellation-sequence is shown in Fig. 4. Note the pronounced banding of the particles or "sites" observed at this rather low strain level. In Fig. 5 some of the JMAK-plots obtained by the tessellation technique are shown. Note that the displacement of the curves along the time axis is irrelevant for this study. As the growth rate is identical in all cases, the relative displacement only reflects the different number of positions that is operative in the tessellation. Included in Fig. 5 is also a curve representing a truly random distribution of points (from Furu [4]). This computer-generated point distribution gives an n value which equals 2, in agreement with the theories on site saturation kinetics and constant growth rate in two dimensions. The real 2D particle distribution from the as-cast material, on the other hand, gives an n value of 1.4. This indicates a spatial particle distribution which deviates from a random distribution. During rolling rearrangement and break-up of the particles occur, and at the exit gauge of hot rolling the n value equals 1.9. This is close to what is expected for a random distribution. In order to investigate the effect of temperature, a couple of samples were cold rolled from the as-cast condition to strain levels being similar with some of the hot rolled samples. The rolling temperature (i.e. hot or cold rolling) did not seem to have any effect on the evolution of the spatial particle distribution, giving

165

similar n-values in cold rolled samples. All the obtained JMAK-exponents are listed in Table 1 including also exponents for tessellation performed on surface locations of hot rolled samples. Note that higher exponents is observed in the surface regions, indicating a spatial particle distribution being closer to random.
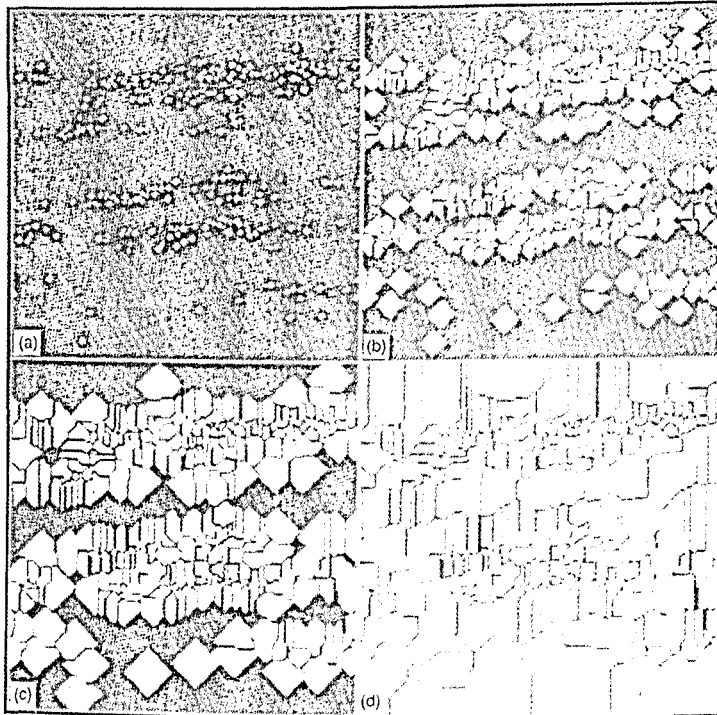

Figure 4. Tessellation-sequence showing different stages in the "transformation" process. Particle pattern from the Al1Mn1Mg alloy, $\bar{\varepsilon} = 2.8$ (centre section of the sheet)

Table 1 : JMAK-exponents obtained for different samples (for details see the text)

Location	As-cast material	$\bar{\varepsilon} = 2.8$	$\bar{\varepsilon} = 3.7$	$\bar{\varepsilon} = 6.2$
n (centre)	1.4	1.5	1.7	1.9
n (surface)	-	1.7	1.8	1.9

Examples of artificial, fully "transformed" structures generated from the tessellation procedure, are shown in Fig. 6a-d. A stronger degree of particle clustering is obvious in early stages of processing. Several such artificially generated structures have been analysed, and the "grain" area distributions were in each case plotted (Fig. 7) based on more than 1200 countings on 4 to 6 different measurement frames. The fully drawn curve in the plots represents the "grain" size distribution in the case of a two dimensional truly random distribution of nucleation sites and site saturation kinetics. These results are obtained from computer simulation on a Cray super computer
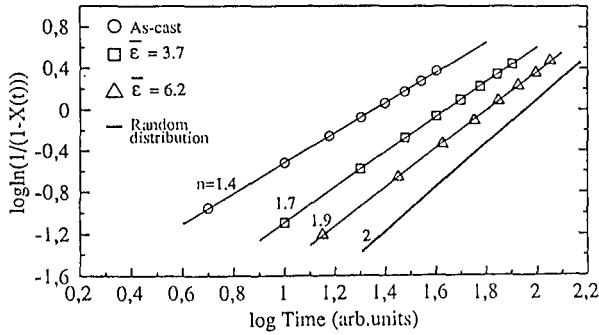
166

Figure 5. JMAK-plots obtained from tessellated microstructures.

(from Furu [4]). It is interesting to note the very good correspondence between this simulated distribution and the distribution obtained from tessellation on the sample taken at a strain of $\bar{\varepsilon}$ = 6.2 (Fig. 7d). Earlier in the processing sequence the distributions are found to be more spread out and they are showing a lower peak intensity (Fig. 7a-c). It is to be noted that the distribution plots obtained from investigation of surface locations, included in Fig. 7b and c, approach the random distribution earlier than the centre location.
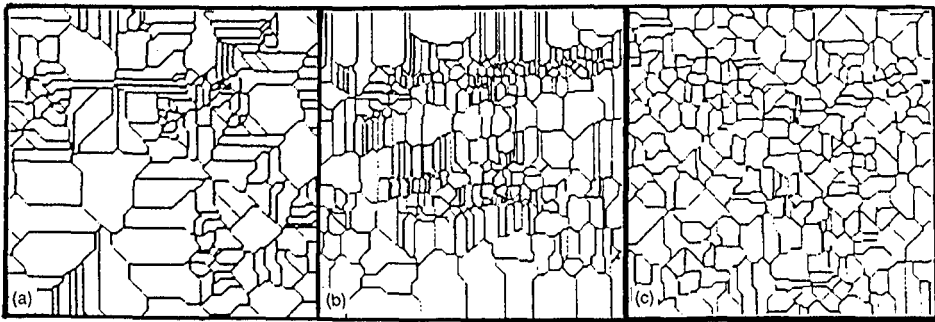

Figure 6. Fully "transformed" microstructures generated form the tessellation procedure.
AlMg1Mn alloy (a) as-cast material, (b) hot rolled to $\bar{\varepsilon}$ = 2.8, (c) hot rolled to $\bar{\varepsilon}$ =6.2

A simple model explaining the development of the spatial particle distribution As mentioned above, a truly random distribution of "nucleation"-sites (or particles) in two dimensions should according to classical JMAK-theory result in an JMAK-exponent which equals 2. Based on the above tessellations a non-randomness parameter, Δn, now may be introduced as follows :

$$\Delta n = n_{random} - n_{obs} \qquad (2)$$

where n_{random}= 2 and n_{obs} represents the JMAK-exponent obtained from the tessellation procedure in each case. The non-randomness parameter therefore can be looked upon as a measure for quantifying the degree of clustering of the particles.
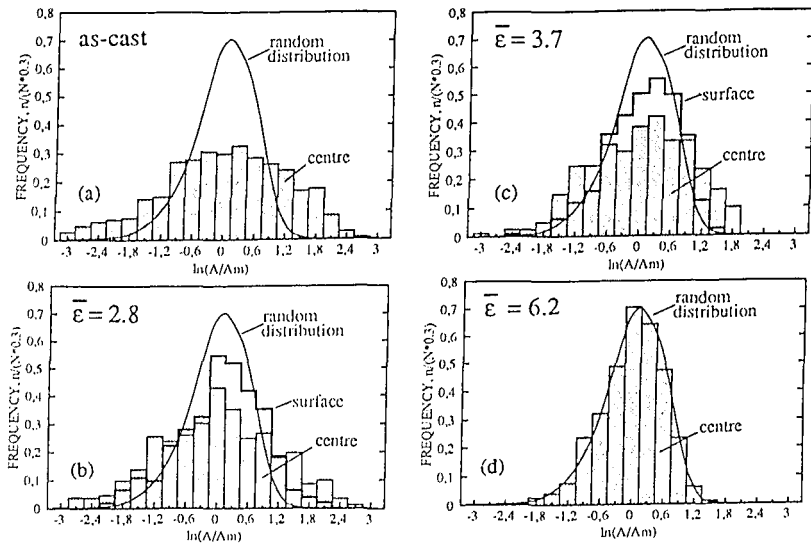
167

Figure 7. Grain area distributions of the tessellated microstructures. Al1Mn1Mg alloy, (a) as-cast material, b) hot rolled to $\bar{\varepsilon} = 2.8$, (c) hot rolled to $\bar{\varepsilon} = 3.7$, (d) hot rolled to $\bar{\varepsilon} = 6.2$. Fully drawn curve represents the grain area distribution in 2 dimensions of a truly random distribution.

Figure 8 shows a plot of the non-randomness parameter for the investigated samples, plotted as a function of equivalent rolling strain. It can be seen that the spatial particle distribution develops towards a close to random distribution at higher strains. A simplified model explaining this observation is shown in Fig. 9. The model assumes that the particles in the as-cast material are located at the cell boundaries, Fig. 9a. During deformation, by either hot or cold rolling, the grains start to deform. At low strains the particles at the cell boundaries will build up in distinct layers, Fig. 9b. However, when the material gets sufficiently deformed the thickness, D, of the flattened-out grains will approach that of the average particle size, η. It seems reasonable that in such a situation the distribution of the particles will be close to that of a random distribution. From the simple model outlined in Fig. 9 the following assumptions can be made concerning the spatial distribution :

$$D > 4\eta \quad , \text{non-random distribution}$$
$$D < \eta \quad , \text{random distribution}$$

By applying the von Mises equivalent strain relation for plane strain deformation ($\bar{\varepsilon}$ $=2/\sqrt{3}\ln Do/D$) the corresponding strain levels can be calculated by substituting the average particle size ($\eta = 2,5$ µm) and the average cell size in the as-cast material (Do= 200 µm). This gives:

$$\bar{\varepsilon} < 3,5 \quad , \text{non-random distribution}$$
$$\bar{\varepsilon} > 5 \quad , \text{random distribution}$$

168

The strain regime 3.5 - 5, which could be regarded as a transition region, is indicated in the plot in Fig. 8. As can be seen this simple model appears to apply well.
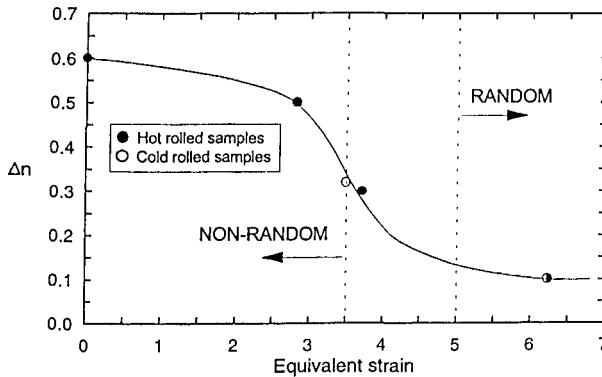

Figure 8. Non-randomness parameter, Δn, for the samples investigated using the tessellation procedure.
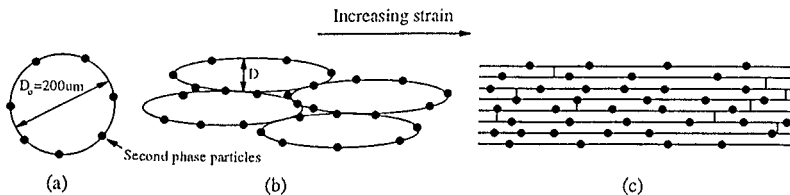

Figure 9. A simple model for the evolution of the spatial particle distribution. (a) particles in the as-cast material are located at the cell boundaries (non-random distribution), (b) at low rolling strain the particles build up in distinct layers (non-random distribution), (c) at high rolling strain the spacing between the particles approaches that of the particle size (close to random distribution).

Conclusions

In the above investigation two independent approaches to explore the two-dimensional spatial particle distribution have been used. Both approaches, JMAK-analysis and size distribution of tessellated structures, show that the spatial distribution is rather inhomogeneous in the early stages of rolling, and develops towards a close to random distribution at higher rolling strains.

References

1. Dirichlet, G., J. Reine angew. Math., 40, 209 (1850).
2. Voronoi, G., J. Reine angew. Math., 134, 198 (1908).
3. Fridy, J. M et al., The 3rd int.conf. on aluminium alloys-ICAA'3, Vol. II, p.333, Trondheim (1992).
4. Furu, T., PhD thesis, Norwegian Institute of Technology, University of Trondheim (1992).